TRPV1 activation in human Langerhans cells and T cells inhibits mucosal HIV-1 infection via CGRP-dependent and independent mechanisms

Jammy Mariotton, Emmanuel Cohen, Aiwei Zhu, Cédric Auffray, Caio César Barbosa Bomfim, Nicolas Barry Delongchamps, Marc Zerbib, Morgane Bomsel, Yonatan Ganor

PNAS RESEARCH ARTICLE | MICROBIOLOGY

TRPV1 activation in human Langerhans cells and T cells inhibits mucosal HIV-1 infection via CGRP-dependent and independent mechanisms

Jammy Mariotton[a,c,1], Emmanuel Cohen[a,c,1], Aiwei Zhu[a,c], Cédric Auffray[b,c], Caio César Barbosa Bomfim[a,c], Nicolas Barry Delongchamps[d], Marc Zerbib[d], Morgane Bomsel[a,c], and Yonatan Ganor[a,c,2]

Edited by Suryaram Gummuluru, Boston University School of Medicine, Boston, MA; received February 28, 2023; accepted April 27, 2023 by Editorial Board Member Stephen P. Goff

Upon its mucosal transmission, HIV type 1 (HIV-1) rapidly targets genital antigen-presenting Langerhans cells (LCs), which subsequently transfer infectious virus to CD4$^+$ T cells. We previously described an inhibitory neuroimmune cross talk, whereby calcitonin gene-related peptide (CGRP), a neuropeptide secreted by peripheral pain-sensing nociceptor neurons innervating all mucosal epithelia and associating with LCs, strongly inhibits HIV-1 transfer. As nociceptors secret CGRP following the activation of their Ca^{2+} ion channel transient receptor potential vanilloid 1 (TRPV1), and as we reported that LCs secret low levels of CGRP, we investigated whether LCs express functional TRPV1. We found that human LCs expressed mRNA and protein of TRPV1, which was functional and induced Ca^{2+} influx following activation with TRPV1 agonists, including capsaicin (CP). The treatment of LCs with TRPV1 agonists also increased CGRP secretion, reaching its anti-HIV-1 inhibitory concentrations. Accordingly, CP pretreatment significantly inhibited LCs-mediated HIV-1 transfer to CD4$^+$ T cells, which was abrogated by both TRPV1 and CGRP receptor antagonists. Like CGRP, CP-induced inhibition of HIV-1 transfer was mediated via increased CCL3 secretion and HIV-1 degradation. CP also inhibited direct CD4$^+$ T cells HIV-1 infection, but in CGRP-independent manners. Finally, pretreatment of inner foreskin tissue explants with CP markedly increased CGRP and CCL3 secretion, and upon subsequent polarized exposure to HIV-1, inhibited an increase in LC–T cell conjugate formation and consequently T cell infection. Our results reveal that TRPV1 activation in human LCs and CD4$^+$ T cells inhibits mucosal HIV-1 infection, via CGRP-dependent/independent mechanisms. Formulations containing TRPV1 agonists, already approved for pain relief, could hence be useful against HIV-1.

CGRP, calcitonin gene-related peptide | CP, capsaicin | HIV-1, human immunodeficiency virus type 1 | LCs, Langerhans cells, T-cells | TRPV1, transient receptor potential vanilloid 1

Significance

Upon its sexual transmission, HIV-1 targets different types of mucosal immune cells, such as antigen-presenting LCs that transfer HIV-1 to its principal CD4$^+$ T cell targets. We previously discovered that calcitonin gene-related peptide (CGRP), a mucosal neuropeptide secreted from pain-sensing peripheral neurons termed nociceptors once activated via their TRPV1 ion channel, strongly inhibits HIV-1 transfer. Herein, we reveal that LCs also express functional TRPV1, whose activation induces secretion of CGRP and the anti-HIV-1 chemokine CCL3, as well as increased HIV-1 degradation, which inhibit LCs-mediated HIV-1 transmission. TRPV1 activation also inhibits direct CD4$^+$ T cell infection, but in CGRP-independent mechanisms. Accordingly, molecules activating TRPV1 could be used to prevent mucosal HIV-1 transmission. This approach represents an original neuroimmune strategy to fight HIV-1.

Mucosal tissues evolved complex strategies to detect and protect our body from external threats and invading pathogens via a bidirectional neuroimmune dialogue between sensory peripheral neurons and mucosal immune cells (1). Pain neurons termed nociceptors, innervating all mucosal epithelia, are specialized in sensing noxious stimuli, such as temperatures above 43 °C and protons/acidic conditions. Their activation is mediated by a large variety of different receptors, of which the nonselective Ca^{2+} ion channel TRPV1 plays a major role (2). Several natural compounds also activate TRPV1, for instance, CP, the spicy component of chili peppers (3); resiniferatoxin (RTX), a naturally occurring chemical found in the cactus-like plant *Euphorbia resinifera* (4); and rutaecarpine (Rut), an alkaloid isolated from the plant *Evodia rutaecarpa* that is used in traditional Chinese medicine to treat cardiovascular diseases (5). As TRPV1-mediated neuronal excitation evoked by CP, but not other TRPV1 agonists, is followed by a long-lasting refractory period with unresponsiveness to additional noxious stimuli (i.e., desensitization), CP topical formulations and skin patches have been approved clinically as analgesics in painful conditions (6).

Upon TRPV1 activation, nociceptors both conduct pain information into the central nervous system and secret neuropeptides locally at the mucosal level (7). Among these is CGRP (8, 9), a potent vasodilator (10) that contributes to the pathophysiology of several disorders (11). Nociceptors are the principal source of secreted CGRP upon TRPV1 activation (7), yet non-neuronal and immune cells also express both molecules (11, 12), e.g. epithelial cells, endothelial cells, fibroblasts, hepatocytes, adipocytes, muscle cells, T cells and dendritic cells (DCs).

CGRP is a key regulator of inflammatory processes, by mediating neurogenic inflammation (13) and also by directly affecting the function of different types of immune cells

The authors declare no competing interest.

This article is a PNAS Direct Submission. S.G. is a guest editor invited by the Editorial Board.

[1]J.M. and E.C. contributed equally to this work.

[2]To whom correspondence may be addressed. Email: yonatan.ganor@inserm.fr.

This article contains supporting information online at https://www.pnas.org/lookup/suppl/doi:10.1073/pnas.2302509120/-/DCSupplemental.

Published May 22, 2023.

in a vasodilator-independent manner (14). For instance, nociceptors associate with LCs, and CGRP shifts LCs-mediated antigen presentation and cytokine secretion from Th1 to Th2/Th17 types (14). Such CGRP-mediated bias towards Th2/Th17 immunity is not limited to LCs and occurs also when additional immune cell types are exposed to CGRP, having both desired and unwanted outcomes during bacterial and fungal infections (15, 16). In contrast, the role of CGRP during viral infections remains largely unexplored.

Mucosal genital epithelia are the principal entry portals during sexual transmission of HIV-1, which rapidly targets LCs in both the vagina (17), and inner foreskin as we reported (18–20), followed by its temporal transfer to $CD4^+$ T cells (21). Investigating the role of CGRP during mucosal HIV-1 infection, we discovered a complex neuroimmune interplay whereby CGRP interacts with LCs and modulates a multitude of cellular and molecular processes, resulting in significant inhibition of LC-mediated HIV-1 transfer (22–25). Accordingly, CGRP enhances expression of atypical double trimmers of langerin (26), the HIV-1-binding LC-specific pathogen-recognition lectin, leading to reduced HIV-1 capture and diversion of HIV-1 from endolysosomes towards efficient proteasomal degradation (24). CGRP also decreases LCs expression of the HIV-1 co-receptor CCR5 (23) and increases LCs secretion of the chemokine CCL3 that binds to CCR5 (22), thus preventing HIV-1 infection of LCs and limiting infection of $CD4^+$ T cells during HIV-1 transfer. Moreover, CGRP blocks increased LC–T cell conjugate formation and subsequent T cell infection, occurring upon polarized inoculation of inner foreskin tissue explants with HIV-1–infected cells ex vivo (22, 25).

Of note, recent studies reported the existence of several epidermal $langerin^+$ cell subsets. Pena-Cruz et al identified vaginal epithelial dendritic cells (VEDCs), expressing both CD1a and langerin but lacking Birbeck granules (BGs) (27); Bertram et al distinguished $CD1a^{high}langerin^{high}$ LCs from CD11c-expressing $CD1a^{low}langerin^{low/neg}$ epidermal dendritic cells (Epi-cDC2s) (28); and Liu et al reported on two steady-state LC subsets, namely $CD1a^{high}langerin^{high}$ LC1 and $CD1a^{low}langerin^{low}$ LC2, with higher CD1c expression and better BGs organization in LC1 vs. LC2 (29). Based on these studies, $CD1a^{high}langerin^{high}$ LCs/LC1 probably represent the same subset, corresponding to "true" LCs. However, as a proportion of Epi-cDC2s expresses langerin in the inner foreskin but only a very low proportion expresses langerin in skin (28), coinciding with the higher frequency of the LC2 subset in inner foreskin compared to skin (29), it remains to be determined whether langerin-expressing Epi-cDC2s and LC2, as well as VEDCs, represent equivalent or distinct LC subsets. Importantly, Epi-cDC2s and VEDCs seem more permissive to HIV-1 compared to LCs (27, 28).

Herein, as we previously reported that LCs secret low basal levels of CGRP that are further increased in an autocrine/paracrine manner by CGRP itself (23), we investigated whether human LCs express functional TRPV1 whose stimulation could induce CGRP secretion, which in turn would prevent HIV-1 transmission. We also studied the functional consequences of TRPV1 activation in $CD4^+$ T cells during HIV-1 infection.

Results

Phenotypic Characterization of LCs. To study TRPV1 expression and function in human LCs, we phenotypically compared LCs within inner foreskin epidermal cell suspensions with monocyte-derived LCs (MDLCs), the latter serving as a complimentary model as the amounts of LCs that can be purified from the inner foreskin are very low. We confirmed the presence of $CD1a^{low}langerin^{neg}$, $CD1a^{low}langerin^{low}$, and $CD1a^{high}langerin^{high}$ subsets within inner foreskin epidermal immune cells, termed herein $langerin^{neg}$ cells, $langerin^{low}$ cells, and $langerin^{high}$ LCs (Fig. 1*A*). As expected (30), differentiation of monocytes into MDLCs resulted in high CD1a expression in >95% of MDLCs and expression of langerin in approximately 30% of MDLCs (Fig. 1*B*). As MDLCs cannot be separated into similar subsets, due to their expression of high and uniform CD1a levels, we gated on all $langerin^+$ MDLCs in our experiments. Of note, langerin expression in MDLCs is a dynamic continuum that can be further increased depending on the in vitro culture conditions (31, 32).

We next investigated by flow cytometry the expression of HIV-1 receptors and co-receptors, including CD4, CCR5 and CD169. These experiments showed that low-moderate (for CD4) and moderate-high (for CCR5) percentages of $langerin^{neg}$ cells, $langerin^{low}$ cells, and $langerin^{high}$ LCs expressed CD4 and CCR5 (Fig. 1 *C–E*), compared to lower percentages in MDLCs (Fig. 1*F*). Of note, we prepared the epidermal cell suspensions using trypsin,

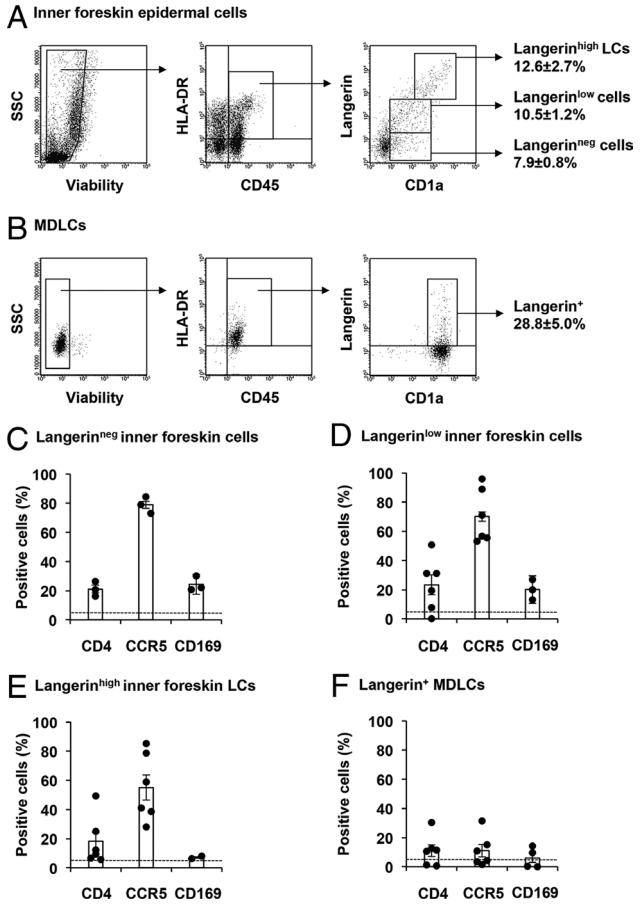

Fig. 1. Gating strategy and phenotypic characterization of inner foreskin LCs and MDLCs. (*A* and *B*) Inner foreskin epidermal cell suspensions (*A*) and MDLCs (*B*) were labeled with Viobility Fixable Dye, stained for surface expression of CD45, HLA-DR, CD1a, and langerin, and examined by flow cytometry. In *A*, cells were separated into $CD1a^{low}Langerin^{neg}$, $CD1a^{low}Langerin^{Low}$ and $CD1a^{high}Langerin^{high}$ subsets. Shown are representative dot plots, with numbers representing mean ± SEM (derived from n = 6 to 10 experiments, using tissue suspensions or MDLCs prepared from different donors) percentages of positive cells, gated on viable $CD45^+HLADR^+$ cells. (*C–F*) Inner foreskin epidermal cell suspensions (*C–E*) and MDLCs (*F*) were further labeled for cell-surface expression of CD4, CCR5, and CD169, and examined by flow cytometry. Shown are mean ± SEM (bars) percentages of positive cells, gated on $langerin^{neg}$ (*C*), $langerin^{low}$ (*D*), $langerin^{high}$ (*E*), and $langerin^+$ (*F*) cells. Each circle represents a distinct experiment using tissues/cells from a different donor.

which cleaves CD4, yet could still detect low CD4 levels. Although not statistically significant ($P = 0.0582$, ANOVA), CCR5 expression in langerin^{high} LCs was reduced compared to langerin^{low} and langerin^{neg} cells, as reported for LCs vs. EpicDCs2 (28). Moreover, low-moderate percentages of langerin^{neg} and langerin^{low} cells expressed CD169 (Fig. 1 *C* and *D*), compared to significantly lower ($P = 0.0209$, ANOVA) and negligible (less than <5%) percentages of both langerin^{high} LCs and MDLCs (Fig. 1 *E* and *F*).

These results show that MDLCs are phenotypically closer to CD1a^{high}langerin^{high} inner foreskin LCs.

LCs Express Functional TRPV1 and CLR. Next, we evaluated the expression of both TRPV1 and calcitonin receptor-like receptor [CLR; one of the components composing the heteromeric CGRP receptor (33)], using antibodies (Abs) directed against extracellular epitopes of human TRPV1 or CLR and validated for flow cytometry. These experiments showed that all three inner foreskin immune cell subsets expressed surface TRPV1 and CLR (Fig. 2*A*), with no significant differences for each receptor expression between langerin^{neg} cells, langerin^{low} cells, and langerin^{high} LCs (65 to 75% for TRPV1 and 70 to 80% for CLR). In comparison, approximately 25% and 35% of langerin^{+} MDLCs expressed surface TRPV1 and CLR (Fig. 2*B*), extending our previous findings showing that MDLCs express mRNA of all three components of the CGRP receptor (22). We also purified mRNA from MDLCs and performed qRT-PCR with TRPV1-specific primers. MDLCs of three different healthy individuals all contained TRPV1 mRNA, which was also amplified from total human brain RNA serving as the positive control (Fig. 2*C*).

To determine whether TRPV1 is functional, MDLCs were loaded with the Ca^{2+} indicator Indo-1, treated with the TRPV1 agonists CP or RTX, and Ca^{2+} influx was measured by flow cytometry. These experiments showed that both TRPV1 agonists induced Ca^{2+} influx in MDLCs in a dose-dependent manner, as did the Ca^{2+} ionophore ionomycin serving as positive control (Fig. 2*D*). We could not perform similar flow cytometry experiments of Ca^{2+} influx with inner foreskin immune cell subsets, due to the limiting amounts of cells that can be purified from these tissues.

These results show that human LCs express functional surface TRPV1, whose activation by TRPV1 agonists induces Ca^{2+} influx.

CP Inhibits HIV-1 Infection In Vitro of MDLCs and CD4^{+} T Cells by Different Mechanisms. To investigate the potential role of TRPV1 during HIV-1 transfer, MDLCs were treated for 24 h with either the TRPV1 agonist CP or CGRP. The cells were then washed, pulsed with HIV-1, washed again, and co-cultured with autologous CD4^{+} T cells. A week later, HIV-1 transfer to and resulting replication in CD4^{+} T cells was determined by measuring the content of the HIV-1 capsid protein p24 in the co-culture supernatants by ELISA. As we reported (22–25), CGRP strongly inhibited MDLCs-mediated HIV-1 transfer in a dose-dependent manner (Fig. 3*A* and *SI Appendix*, Fig. S1*A*). Treatment with CP also inhibited HIV-1 transfer in a dose-dependent manner, but with lower efficiency and potency compared to CGRP (Fig. 3*A* and *SI Appendix*, Fig. S1*B*). To confirm that CP-induced inhibition was mediated via activation of TRPV1, MDLCs were pretreated with the TRPV1 antagonist A425619 (34) before addition of CP, and HIV-1 transfer was determined as above. The TRPV1 antagonist alone had little effect on HIV-1 transfer, but completely abrogated CP-mediated inhibition (Fig. 3*B*). Of note, treatment of MDLCs with ethanol (i.e., utilized as diluent, at 0.1% for the highest concentrations of CP we used) that also activates TRPV1 (35) had no effect (Fig. 3*B*).

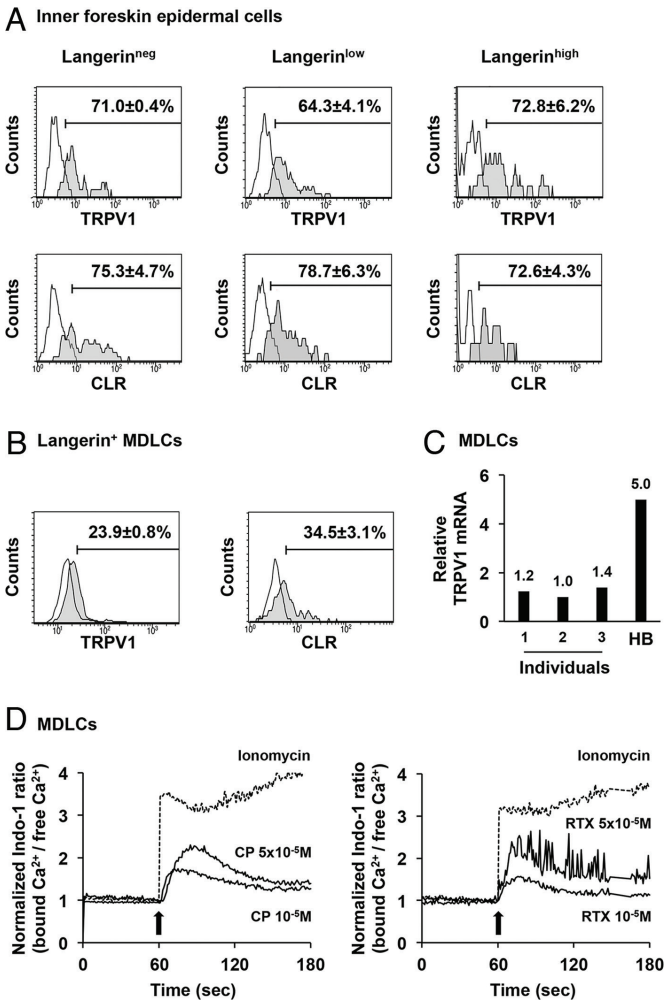

Fig. 2. LCs express functional TRPV1 and CLR. (*A* and *B*) Inner foreskin epidermal cell suspensions (*A*) and MDLCs (*B*) were stained for surface expression of TRPV1 and CLR, and examined by flow cytometry. Representative overlays show TRPV1 and CLR expression (grey histograms) vs. matched isotype controls (line histograms), in epidermal cells and MDLCs gated as show in Fig. 1. Numbers represent mean ± SEM percentages of positive cells (derived from n = 3 to 6 experiments, using tissues/cells from different donors). (*C*) Relative TRPV1 mRNA expression in MDLCs from three different human individuals (1 to 3) normalized to beta actin, with total human brain (HB) mRNA serving as positive control. (*D*) MDLCs were loaded with the Ca^{2+} indicator Indo-1 and examined over time by flow cytometry. Representative graphs (n = 3) show the normalized bound/free Ca^{2+} ratio, indicative of Ca^{2+} influx, at baseline (t = 0 s, set to 1) and following treatment (t = 60 s, arrow) with the indicated concentrations of CP (*Left*) or RTX (*Right*). Ionomycin (1 μM; broken lines) served as positive control.

Next, to explore the interplay between TRPV1 activation and CGRP secretion, MDLCs were treated for 24 h with the TRPV1 agonists CP and Rut, and the levels of secreted CGRP were immediately determined in the culture media. Treatment with both TRPV1 agonists increased CGRP secretion from MDLCs in a dose-dependent manner reaching 10^{-11} to 10^{-10}M (Fig. 3*C*), which is within the range of concentrations for HIV-1 transfer inhibition by CGRP (Fig. 3*A*). As positive control, cells were also treated with exogenous CGRP followed by extensive washing and culture for additional 24 h, in order to induce autocrine/paracrine CGRP secretion from MDLCs as we reported (23), which we reconfirmed herein (Fig. 3*C*). To further determine whether CP-induced CGRP secretion is responsible for HIV-1 transfer inhibition, MDLCs were pretreated with the CGRP receptor antagonist BIBN4096 (36) before addition of CP or CGRP. The CGRP receptor antagonist alone had little effect on HIV-1

transfer, but abrogated partially CP-mediated and completely CGRP-mediated inhibition (Fig. 3*D*).

To identify the mechanisms by which CP inhibits HIV-1 transfer via secreted CGRP (at least to some extent), we tested whether CP induces the CGRP-mediated anti-HIV-1 functions that we previously identified in MDLCs, namely increased CCL3 secretion, efficient HIV-1 degradation, and modulation of langerin and CCR5 expression (22–25). These experiments showed that a CCL3 neutralizing Ab abrogated CP-induced inhibition, alike for CGRP, indicating that both CP and CGRP induced CCL3 secretion from MDLCs that inhibited HIV-1 transfer (Fig. 3*E*). In addition, HIV-1 intracellular contents in MDLCs were lower following treatment with CP and CGRP, indicating that both increased HIV-1 degradation (Fig. 3*F*). In contrast, CP had no effect on langerin and CCR5 expression levels, which were increased and decreased, respectively, by CGRP (*SI Appendix*, Fig. S2). Of note, we previously reported that CGRP has no effect on DC-SIGN that is expressed by MDLCs (22), which we also observed following CP treatment [mean ± SEM (n = 4) percentages of 90.1 ± 2.0 vs. 90.1 ± 1.8, for DC-SIGN$^+$ untreated vs. CP-treated cells].

Finally, we studied the effects of CP and CGRP on CD4$^+$ T cells. First, using CD4$^+$ T cells purified from blood or contained within inner foreskin epidermal cell suspensions, we found by flow cytometry that the cells expressed both TRPV1 and CLR (*SI Appendix*, Fig. S3). Second, we found that CP, but not CGRP, inhibited direct infection of primary blood CD4$^+$ T cells with HIV-1 in a dose-dependent manner (Fig. 3*G*). Importantly, CP did not affect T cell activation (i.e., that is required for in vitro infection of T cells with HIV-1), as addition of CP to CD4$^+$ T cells during their activation had no effect on surface expression of the T cell activation markers CD25 and CD69 [mean ± SEM (n = 3) percentages of 29.3 ± 5.0 vs. 25.0 ± 4.6 CD25$^+$ cells and 33.3 ± 8.2 vs. 30.1 ± 7.0 for CD69$^+$ cells; untreated vs. CP-treated primary blood CD4$^+$ T cells].

Together, these findings show that TRPV1 activation in MDLCs inhibits HIV-1 transfer via both CGRP-dependent/independent mechanisms. TRPV1 activation also directly inhibits HIV-1 infection in CD4$^+$ T cells, only in CGRP-independent manners.

CP Induces CGRP and CCL3 Secretion and Inhibits HIV-1 Infection in Inner Foreskin Mucosal Tissues Ex Vivo. To extend the in vitro findings above, we tested the activity of CP using mucosal tissues and successive steps (Fig. 4*A*), based on our previously established experimental protocol (18). Inner foreskin tissue explants were first submerged in culture media and left untreated or pretreated for 24 h with CP. The media were then collected and ELISA kits were used to measure the levels of secreted CGRP and CCL3. Next, the explants were transferred to two-chamber transwell inserts and inoculated in a polarized manner for a short time period of 4 h with either noninfected or HIV-1–infected cells. Of note, we previously showed that whereas mucosal infection by cell-free virus is not efficient, HIV-1–infected cells form viral synapses with the apical surface of keratinocytes (18). In the inner foreskin, viral synapse formation induces in turn secretion of thymic stromal lymphopoietin 1 (TSLP1), mediating epidermal redistribution of LCs that rapidly internalize incoming HIV-1 (20), i.e., cell-free HIV-1 penetrating the tissue after its local production at the viral synapse, but not the inoculated HIV-1–infected cells themselves. In parallel, viral synapse formation induces secretion of the T cell chemokine CCL5, mediating recruitment of T cells from the dermis into the epidermis (19). These processes facilitate increased formation of LC–T cell conjugates,

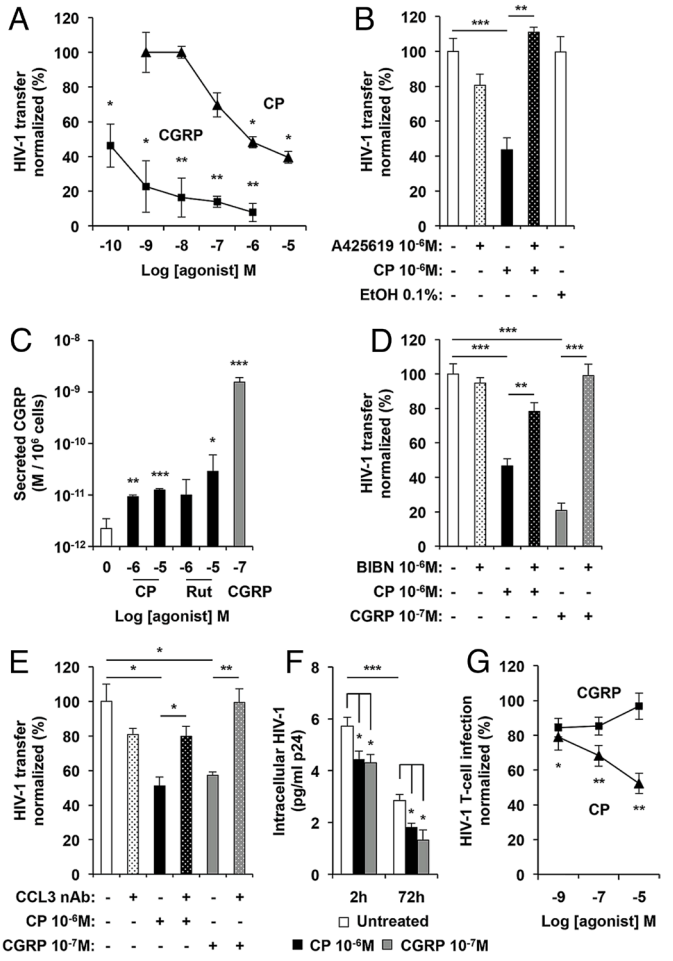

Fig. 3. TRPV1 activation in MDLCs and CD4$^+$ T cells inhibits HIV-1 transfer and infection in vitro. (*A*, *B*, *D*, and *E*) MDLCs were treated for 24 h with the indicated molar concentrations of CP or CGRP. The TRPV1 antagonist A425619 (*B*) and the CGRP receptor antagonist BIBN4096 (*D*) were added 15 min before addition of CP or CGRP. The cells were then washed, pulsed with HIV-1 for 4 h, washed again, and cocultured with autologous CD4+ T cells. In some experiments, a CCL3 neutralizing Ab was added during the co-culture period (*E*). HIV-1 replication was evaluated a week later by measuring p24 content in the co-culture supernatants using ELISA. Shown are mean ± SEM (n = 3 to 4) percentages of HIV-1 transfer, normalized against untreated cells serving as the 100% set point. (*C*) MDLCs were treated for 24 h with the indicated molar concentrations of CP, Rut or CGRP. Culture supernatants were collected immediately after CP and Rut treatment, or following extensive washing and culture in fresh medium for additional 24 h after CGRP treatment, and an EIA was used to measure CGRP levels. Shown are mean ± SEM (n = 3) levels of secreted CGRP per 10^6 MDLCs. (*F*) MDLCs were treated for 24 h with CP or CGRP, washed and pulsed with HIV-1 for 2 h. The cells were next washed again, treated immediately or 72 h later with trypsin for 10 min to remove surface-bound virus, lysed, and intracellular HIV-1 was measured in the cell lysates using p24 ELISA. Shown are mean ± SEM (n = 4) concentrations of intracellular HIV-1 p24. (*G*) PHA/IL-2-activated blood primary CD4$^+$ T cells were treated for 24 h with the indicated molar concentrations of CP or CGRP. The cells were then washed, pulsed with HIV-1 for 4 h, washed again, and HIV-1 replication was evaluated 3 d later by p24 intracellular staining and flow cytometry. Results (n = 5 to 8) are shown as in *A*. In all graphs, **P* < 0.0500, ***P* < 0.0050, ****P* < 0.0005, Student's *t*-test.

permitting subsequent epidermal transfer of infectious HIV-1 from LCs to T cells, and subsequent T cell exit into the dermis (18). In contrast, cell-free HIV-1 fails to induce such changes at this early time point (18), although free virions might penetrate the inner foreskin at later time points of ≥24 h post infection when using a cell-free inoculum (37).

Accordingly, the CP-treated (and CGRP-treated as positive control) and untreated inner foreskin explants were digested with dispase and trypsin, immediately after viral pulse and washing, to

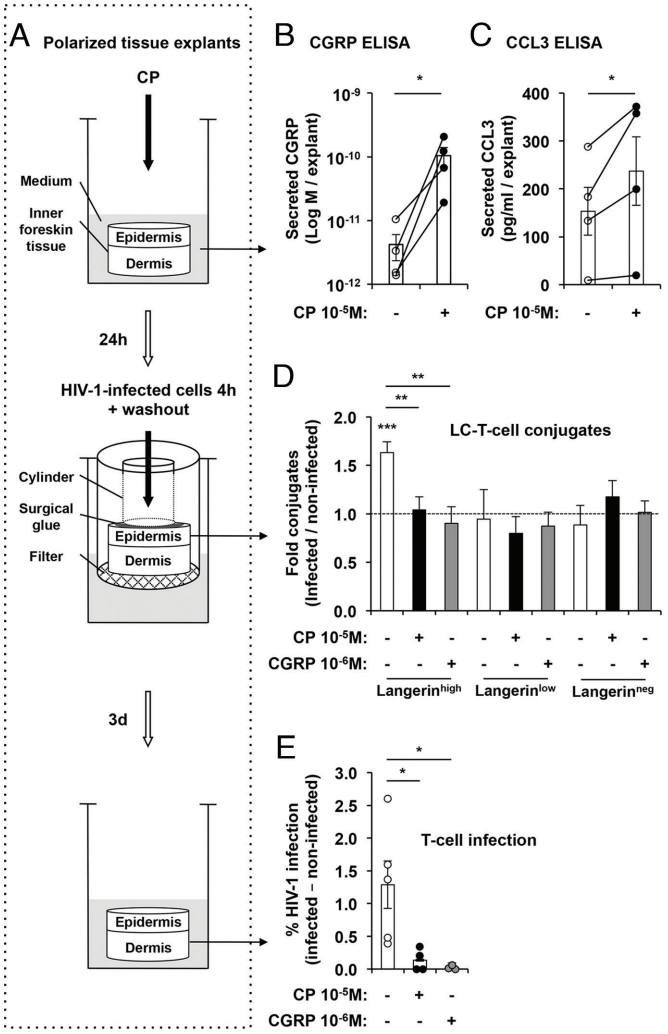

Fig. 4. CP inhibits HIV-1 infection in mucosal inner foreskin tissues ex vivo. (*A*) Schematic representation of the different experimental steps. Inner foreskin tissue explants were submerged in culture media, left untreated or pretreated with CP, and media were collected 24 h later (*Top*). Explants were next washed, transferred to two-chamber transwell inserts and inoculated in a polarized manner with either noninfected or HIV-1–infected cells. Following 4 h inoculation, the cell-associated HIV-1 inoculum was washed out, and the explants were immediately digested with dispase and trypsin to obtain epidermal cell suspensions (*Middle*). Other explants were further incubated for additional 3 d submerged in fresh culture media, before digestion with collagenase and DNase to obtain dermal cell suspensions (*Bottom*). (*B* and *C*) Secreted levels of CGRP (*B*) and CCL3 (*C*) in 24 h culture media of inner foreskin explants, measured using CGRP and CCL3 ELISA. Shown are mean ± SEM (bars) from n = 4 explants per condition (for each individual), in matched untreated (open circles) or CP-treated (closed circles) explants; **P* = 0.0286 (for CGRP) and **P* = 0.0199 (for CCL3), Mann–Whitney *U* test. (*D*) In epidermal suspensions, after gating out cell debris and $FSC^{highest}SSC^{highest}$ keratinocytes, cells were further gated on $CD3^{+}CD8^{-}$ T cells, and the percentages of FSC^{high} conjugates with $CD1a^{high}Langerin^{high}$, $CD1a^{low}Langerin^{Low}$ and $CD1a^{low}Langerin^{neg}$ subsets were determined by flow cytometry. Shown are mean ± SEM (n ≥ 3) folds increase in conjugate formation, calculated as [(% conjugates following inoculation with HIV-1–infected PBMCs)/(% conjugates following inoculation with noninfected PBMCs). (*E*) In dermal suspensions, cells were gated on $FSC^{low}SSC^{low}$ lymphocytes, and the percentages of $CD3^{+}p24^{+}$ cells were determined. Shown are mean ± SEM (n = 3) percentages of HIV-1–infected T cells, calculated as [(%$CD3^{+}p24^{+}$ cells following inoculation with HIV-1–infected PBMCs) − (%$CD3^{+}p24^{+}$ cells following inoculation with noninfected PBMCs)]. In *D* and *E*, **P* < 0.0500, ***P* < 0.0050, ****P* < 0.0005, Student's *t* test.

obtain epidermal cell suspensions and determine by flow cytometry the formation of epidermal LC–T cell conjugates. In other experiments, the explants were washed, further incubated for 3 d submerged in fresh culture medium, and then digested with collagenase and DNase to obtain dermal cell suspensions and determine by flow cytometry the resulting infection of T cells with HIV-1.

In untreated inner foreskin tissue explants, baseline secretion levels were in the range of 10^{-12} to 10^{-11}M for CGRP (Fig. 4*B*; mean ± SEM of 4.2 ± 1.9 × 10^{-12}M), and 10 to 300 pg/mL for CCL3 (Fig. 4*C*; mean ± SEM of 153.6 ± 50.1 pg/mL). In all matched explants, CP treatment significantly increased secretion of CGRP (Fig. 4*B*; mean ± SEM of 1.2 ± 0.4 × 10^{-10} M, approximately ×30 fold increase) and CCL3 (Fig. 4*C*; mean ± SEM of 237.2 ± 71.4 pg/mL, approximately ×1.5 fold increase).

We then determined upon inoculation with HIV-1–infected cells (i.e., that are washed out following inoculation and do not enter the tissue), which cell subset forms conjugates with resident/recruited T cells, and found increased formation of high forward scatter (FSC) conjugates with $langerin^{high}$ LCs, but not $langerin^{low}$ or $langerin^{neg}$ cells (Fig. 4*D*). Pretreatment with CP, and with CGRP as positive control, completely abrogated the increased formation of these $langerin^{high}$ LC–T cell conjugates (Fig. 4*D*). In addition, inoculation with HIV-1–infected cells resulted in T cell infection, which was almost completely prevented by pretreatment with either CP or CGRP (Fig. 4*E*).

These findings show that CP induces CGRP and CCL3 secretion and inhibits HIV-1 transmission in mucosal tissues ex vivo.

Discussion

We report herein on a novel neuroimmune mechanism that limits mucosal HIV-1 infection, whereby TRPV1 activation in vitro in human LCs leads to secretion of CGRP, which in turn inhibits LCs-mediated HIV-1 transfer to T cells. Similar TRPV1 activation in human T cells also inhibits their HIV-1 infection, but in CGRP-independent mechanisms. In inner foreskin tissues ex vivo, the net outcome following pretreatment with both CP and CGRP is almost complete inhibition of increased LC–T cell conjugate formation and subsequent T cell infection, yet we speculate that the underlying mechanisms differ. Hence, CGRP efficiently blocks conjugate formation, to prevent ensuing T cell infection. In contrast, CP-mediated effects could be attributed to a block of LCs-mediated HIV-1 transfer, coupled to direct inhibition of T cell infection.

TRPV1 immunoreactivity in human skin LCs was previously reported by one study (38) but was not confirmed by another study (39). In addition, mouse and human $CD4^{+}$ T cells were reported to express functional surface TRPV1 (40). We used both qRT-PCR and immunolabeling followed by flow cytometry, to show that human MDLCs and primary blood $CD4^{+}$ T cells, as well as inner foreskin $langerin^{low}$, $langerin^{neg}$, $langerin^{high}$, and $CD3^{+}CD8^{-}$ T cells express TRPV1 mRNA and/or surface protein. Whether TRPV1 activation in immune cells leads to desensitization, alike for nociceptors (2), remains an open question.

CGRP is expressed by approximately 45% of dorsal root ganglia nociceptor neurons, predominantly in small diameter unmyelinated C-fibers, as well as small-to-medium diameter Aδ fibers (41). About half of these CGRP-expressing nociceptors, which innervate all mucosal epithelia including the inner foreskin, also express TRPV1 and respond to noxious stimuli and natural TRPV1 agonists by secreting CGRP (42). We show that a similar sensory mechanism operates in LCs, which secret CGRP following TRPV1 activation. In fact, we speculate that CP induces some, but not all, CGRP-mediated anti-HIV-1 effects in LCs as a result of its capacity to induce secretion of only low levels of CGRP, which nevertheless are within its effective anti-HIV-1 range. These results are the first to demonstrate a role for TRPV1 in LCs, and extend previous observations of a similar interplay between

TRPV1 and CGRP in other non-neuronal cells, e.g., TRPV1 activation in keratinocytes (43) and DCs (44) is linked to CGRP release.

Based on our previous quantitative analysis of cellular densities in the inner foreskin (18, 19), we could estimate that each explant used herein will contain approximately 10^6 langerin$^+$ cells. As treatment with 10^{-5}M CP induces secretion of approximately 10^{-11}M CGRP from such amount of MDLCs (Fig. 2*C*), compared to 10^{-10}M CGRP per explant (Fig. 4*B*), resident LCs within the tissue explants could contribute approximately 10% of total secreted CGRP upon CP activation. The remaining 90% most probably originate from nociceptors, which we speculate to still maintain their capacity to respond to TRPV1 agonists by releasing CGRP that is prestored in their mucosal nerve terminals, although nociceptors are sectioned during tissue sampling. In addition, foreskin keratinocytes could represent another source of CGRP, which can be secreted from these cells upon TRPV1 activation by CP (12). It would be instrumental now to evaluate the exact contribution of nociceptors and keratinocytes to CP-induced mucosal CGRP secretion, and determine whether and how LCs participate in the mucosal sensory network.

Our results further extend our previous findings, by showing that langerin^{high} inner foreskin LCs are the ones forming conjugates with T cells upon HIV-1 inoculation. Whether such function is related to their epidermal distribution closer to the apical surface, differential expression profile of adhesion molecules and lower permissiveness to HIV-1 (28), or only represents an early temporal snapshot of mucosal HIV-1 transmission, remains to be determined. Interestingly, all three cell subsets we investigated expressed CLR, yet our recent study showed that only langerin^{high} LCs were affected by CGRP during mucosal infection with herpes simplex virus (26). As langerin$^{low/neg}$ cells transcriptionally resemble DCs and not LCs (28, 29), the lack of CGRP inhibitory effects in these cell subsets might correlate with our previous observations that CGRP has no effect on DCs-mediated HIV-1 transfer to T cells (22).

Our previous studies also showed that pretreatment with CGRP of CD4$^+$ T cells, rather than LCs, has no effect on HIV-1 transfer (22). Similarly, our recent in vivo study suggests that CGRP acts by targeting LCs and delaying HIV-1 dissemination to CD4$^+$ T cells in humanized mice (25). These findings indicate that CGRP acts on LCs and not T cells, to inhibit HIV-1 transfer. Indeed, although T cells are responsive to both CP and CGRP, and express TRPV1 and CLR as reported herein and by others (40, 45, 46), we show that CP, but not CGRP, directly inhibits HIV-1 infection of CD4$^+$ T cells. Such inhibition is not a result of decreased T cell activation, as we found no differences in the expression of activation markers in CP-treated vs. untreated CD4$^+$ T cells. These results contrast with a previous study that identified TRPV1 as a component of the T cell receptor (TCR) complex, in which TRPV1 inhibition was associated with decreased Ca^{2+} influx, TCR signaling, and T cell activation (40). We speculate that these discrepancies might be related to the different methods used in each study for T cell activation [i.e., phytohaemagglutinin (PHA) vs. anti-CD/CD28 Abs] and TRPV1 modulation (i.e., activation with agonists vs. blocking with antagonists). The exact CGRP-independent mechanisms, which underlie CP-induced inhibition of T cell HIV-1 infection, remain to be determined.

Formulations containing CP are clinically approved for local pain control. For instance, topical CP is used to treat HIV-1-associated distal sensory polyneuropathy and postherpetic neuralgia (6), and CP creams are applied vaginally to treat vulvar vestibulitis syndrome (47) although their distressing and debilitating effects in this condition should not be underestimated (48). Indeed, as CP is a known irritant, its topical application induces an initial burning "flare" sensation associated with nociceptor activation. Such discomfort is limited to the site of application and resolves after the first few days (6). On-going studies are exploring strategies to improve CP bioavailability (e.g. CP nanoparticles), which may decrease CP dosage, leading to minimal side effects (49). Of note, the effective anti-HIV-1 concentration of CP we report herein is much lower compared to low-concentration CP topical formulations that contain 1% (≈30 mM) CP.

Together, our study provides "proof of concept" and support for the clinical use of formulations containing CGRP and/or TRPV1 agonists as novel topical microbicides active against HIV-1 in the male genitals. Whether these would be useful also during HIV-1 transmission in the female genitals remains to be determined. This neuroimmune based approach offers an original and potentially advantageous alternative for prevention of HIV-1 transmission.

Materials and Methods

Cells and Tissues. Peripheral blood mononuclear cells (PBMCs) from healthy HIV-1 seronegative individuals were separated from whole blood by standard Ficoll gradient. CD14$^+$ monocytes and CD4$^+$ T cells were purified from PBMCs by negative magnetic selection (Stemcell Technologies). Monocytes (1×10^6/well, in 12-well plate) were differentiated into MDLCs (30) in complete medium [RPMI 1640 medium, 10% fetal bovine serum (FBS), 2 mM glutamine, 100 U/mL penicillin and 100 μg/mL streptomycin (Gibco Invitrogen)] supplemented with 100 ng/mL granulocyte-macrophage colony-stimulating factor (GM-CSF), 10 ng/mL interleukin 4 (IL-4) and 10 ng/mL transforming growth factor beta 1 (TGFb1) (R&D systems), and used between days 7 to 9 of differentiation.

Normal foreskin tissues were obtained from healthy adults undergoing circumcision (Urology Service, Cochin Hospital, Paris), under informed consent and ethical approval (Comités de Protection des Personnes CPP Paris-IdF XI, N.11016). Inner foreskins (distinguished by their lighter color and morphology) were separated mechanically, and remaining fat and muscle tissue was removed from the dermal side. Epidermal cell suspensions were prepared as we described (18, 19). Briefly, tissue pieces were incubated with their epidermal side facing up in RPMI 1640 medium supplemented with 2.4 U/mL Dispase II (Roche Diagnostics GmbH) overnight at 4 °C. The epidermis and dermis were then mechanically separated using forceps and epidermal cell suspensions were prepared by incubating the epidermal sheets in 0.05% Trypsin/EDTA (Gibco Invitrogen) for 10 min at 37 °C, followed by inactivation of trypsin with FBS, mechanical disruption using a 10-mL pipette, filtration of released cells through 100 μm nylon cell strainers and centrifugation.

Virus and Infected Cells. Viral stocks of the HIV-1 molecular clones ADA and JRCSF or the primary isolate 93BR029 (V29), all clade B and CCR5-tropic (NIH AIDS reagent program) were prepared by transfection of 293T cells or by amplification on PHA/IL-2-stimulated PBMCs, respectively, and quantified using the p24 Innotest HIV-1 ELISA (Fujirebio). PBMCs highly infected with HIV-1 V29 were prepared as we reported (18).

Flow Cytometry. MDLCs, primary CD4$^+$ T cells (1×10^5/well) or inner foreskin epidermal cells (5×10^5/well), in duplicates in round bottom 96-well plate, were stained for 30 min on ice in a final volume of 50 μL phosphate-buffered saline (PBS). The following Abs were used: pacific orange (PO)–conjugated mouse–antihuman CD45 (clone HI30, 1:100; Gibco Invitrogen); allophycocyanin (APC)-H7–conjugated mouse–antihuman HLD-DR (clone G46-6, 1:100; BD Pharmingen); APC or phycoerythrin (PE)–conjugated mouse–antihuman CD1a (clone HI149, 1:10; Pharmingen); APC or PE–conjugated recombinant human–antihuman langerin [clone REA770 (equivalent to clone DCGM4), 1:100; Miltenyi Biotec, Paris, France]; PE–conjugated mouse–antihuman CD8 (clone HIT3a, 1:10; Pharmingen); fluorescein isothiocyanate (FITC)–conjugated mouse–antihuman CD3 (clone HIT3a, 1:10; Pharmingen), CD4 (clone RPA-T4 1:10; Pharmingen),

CCR5 (clone 2D7, 1:10; Pharmingen) or CD169 (clone 7-239, 1:20; Miltenyi); FITC–conjugated rabbit–antihuman TRPV1 or CLR (1:25; Alomone Labs). Viability was determined using the Viobility Fixable Dye staining kit (Miltenyi), according to the manufacturer's instructions. Fluorescent profiles were acquired using a Guava easyCite and analyzed with the InCyte software (Merck-Millipore).

TRPV1 qRT-PCR. RNA purification from MDLCs and cDNA reverse transcription were performed as we previously described (23). Total human brain (HB) RNA (Clontec) served as positive control. qRT-PCR was performed with the TRPV1 TaqMan Gene Expression Assay (TheroFisher Scientific). The 20 μL PCR mixture contained 2 μL of cDNA prepared from 1 μg total RNA, 10 μL of Master Mix 2X from TaqMan RNA-to-Ct *1-step* Kit (TheroFisher Scientific), and 1 μL of each primer. Reactions were performed in triplicates, with beta-actin as the internal control. Thermocycler conditions consisted of preincubation at 95 °C for 10 min for 1 cycle, followed by 45 cycles of denaturation at 95 °C for 15 s and annealing/extension at 60 °C for 60 s. Amplification, data acquisition, and analysis were carried out using the LightCycler 480 Software (Roche) and relative expression levels were quantified using the $2^{-\Delta Ct}$ method.

Intracellular Ca^{2+}. MDLCs (4×10^5/tube) were loaded for 30 min at 37 °C with 1 μM of the membrane-permeable fluorescent Ca^{2+} indicator dye Indo-1 AM, washed, equilibrated for 5 min at 37 °C before acquisition, and Ca^{2+} traces were recorded by flow cytometry using an LSR-II (BD Biosciences), as we reported (50). After the establishment of a stable baseline for 60 s, cells were stimulated with the indicated concentrations of CP, RTX, or ionomycin (Sigma), and traces were recorded for an additional 120 s. Data were analyzed with Diva software (BD Biosciences).

HIV-1 Degradation, Transfer, and Infection. MDLCs (1×10^5/well) were treated for 24 h at 37 °C with the indicated concentrations of CP, CGRP (Sigma), and absolute ethanol in triplicates in a 96-well round-bottom plate (200 μL/well final). When indicated, The TRPV1 antagonist A425619 (Tocris/Biotechne) and the CGRP receptor antagonist BIBN4096 (Sigma) were added 15 min before agonists. Of note, we verified that at the concentrations used herein, none of the agonists and antagonists affected cell viability. The cells were then washed and pulsed with HIV-1 ADA (1 ng p24 corresponding to multiplicity of infection of 0.2) for 2 to 4 h at 37 °C. For HIV-1 intracellular content as we reported (24), cells were washed, incubated with trypsin-EDTA (Gibco) for 10 min at 37 °C to remove surface-bound virus either immediately after viral pulse or 72 h later, lysed with NP-40, and HIV-1 contents were measured in the cell lysates using a p24 ELISA (Fujirebio). For HIV-1 transfer, cells were washed and incubated with autologous $CD4^+$ T cells (3×10^5/well). In some experiments, a neutralizing CCL3 goat Ab (R&D Systems) was added at 1 μg/mL during the coculture period, as before (22). HIV-1 p24 content was measured a week later in the coculture supernatants using p24 ELISA.

Blood primary $CD4^+$ T cells were first activated for 48 h with 5 μg/mL PHA (Sigma) + 48 h with 10 U/mL IL-2 (Roche), followed by treatment with the indicated concentrations of CP and CGRP for 24 h. Cells were then pulsed with HIV-1 JRCSF (10 ng p24/well) for 4 h at 37 °C and washed. After 3 d, cells were fixed, permeabilized, stained for 30 min at room temperature with PE–conjugated mouse–antihuman Ab to HIV-1 p24 and core antigens (clone KC57, 1:160; Beckman Coulter), and examined by flow cytometry as above.

Inner Foreskin Tissue Explants. Round inner foreskin tissue pieces were cut using a 8-mm–diameter Harris Uni-Core, transferred to 24-well plate and incubated submerged for 24 h at 37 °C in 1 mL complete RPMI medium, alone or supplemented with 10^{-5}M CP or 10^{-6}M CGRP (four explants per condition). The media were next collected and tested for CGRP and CCL3 content (see below). Next, the tissues were washed, transferred to two-chamber transwell inserts (Sigma), and inoculated in a polarized manner for 4 h at 37 °C with either noninfected or HIV-1–infected PBMCs (in duplicates), as we described (18, 19). Epidermal cell suspensions were prepared immediately after inoculation, as described above. Dermal cell suspensions were prepared following washing of the explants, additional incubation for 3 d at 37 °C submerged in 1 mL fresh medium, and subsequent enzymatic digestion with collagenase and DNase, as we described (18, 19). Pooled cells of each duplicate were resuspended in PBS, transferred to a 96-well round-bottom plate, stained for 30 min on ice with the Abs described above, and examined by flow cytometry.

CGRP and CCL3 Secretion. MDLCs (5×10^5/well) were treated for 24 h at 37 °C with the indicated concentrations of CP, Rut and CGRP in a 96 round-bottom wells plate (200 μL/well final). The culture supernatants were collected immediately following CP and Rut treatment or following extensive washing and incubation for additional 24 h at 37 °C in fresh medium following CGRP treatment. CGRP levels were determined using a competitive CGRP enzyme immunoassay (EIA; Peninsula, San Carlos, CA). Secretion from inner foreskin tissue explants into the culture media was determined using direct ELISA for CGRP (Bertin, Rockville, MD) and CCL3 (R&D systems).

Statistical Analysis. Statistical significance was analyzed with the two-tailed Student's *t* test. For comparing secreted CGRP and CCL3 levels from matched tissue explants, pairwise comparisons were performed with the nonparametric Mann–Whitney *U* test.

Data, Materials, and Software Availability. All study data are included in the article and/or *SI Appendix*.

ACKNOWLEDGMENTS. J.M. and E.C. were supported by PhD fellowships from the French national agency for HIV-1 and hepatitis research (ANRS|MIE), A.Z. was supported by a PhD fellowship from the Chinese scientific council, C.C.B.B. was supported by a postdoctoral fellowship from SIDACTION, and the study was funded by a grant to Y.G. from SIDACTION (Aide aux Equipes, Ref 17-2-AEQ-11613).

Author affiliations: [a]Laboratory of Mucosal Entry of HIV-1 and Mucosal Immunity, Department of Infection Immunity and Inflammation, Cochin Institute, F-75014 Paris, France; [b]Laboratory of Regulation of T Cell Effector Functions, Department of Infection Immunity and Inflammation, Cochin Institute, F-75014 Paris, France; [c]Université Paris Cité, Institut Cochin, INSERM U1016, CNRS UMR8104, F-75014 Paris, France; and [d]Urology Service, Groupe Hospitalier (GH) Cochin-St Vincent de Paul, F-75014 Paris, France

Author contributions: C.A. and Y.G. designed research; J.M., E.C., A.Z., C.A., C.C.B.B., and Y.G. performed research; N.B.D. and M.Z. contributed new reagents/analytic tools; J.M., E.C., A.Z., C.A., C.C.B.B., and Y.G. analyzed data; and M.B. and Y.G. wrote the paper.

1. S. Talbot, S. L. Foster, C. J. Woolf, Neuroimmunity: Physiology and pathology. *Annu. Rev. Immunol.* **34**, 421–447 (2016).
2. B. Nilius, A. Szallasi, Transient receptor potential channels as drug targets: From the science of basic research to the art of medicine. *Pharmacol. Rev.* **66**, 676–814 (2014).
3. M. J. Caterina *et al.*, The capsaicin receptor: A heat-activated ion channel in the pain pathway. *Nature* **389**, 816–824 (1997).
4. A. Szallasi, P. M. Blumberg, Resiniferatoxin, a phorbol-related diterpene, acts as an ultrapotent analog of capsaicin, the irritant constituent in red pepper. *Neuroscience* **30**, 515–520 (1989).
5. S. Jia, C. Hu, Pharmacological effects of rutaecarpine as a cardiovascular protective agent. *Molecules* **15**, 1873–1881 (2010).
6. O. M. Hall *et al.*, Novel agents in neuropathic pain, the role of capsaicin: Pharmacology, efficacy, side effects, different preprations. *Curr. Pain Headache Rep.* **24**, 53 (2020).
7. F. De Logu, R. Nassini, L. Landini, P. Geppetti, Pathways of CGRP release from primary sensory neurons. *Handb Exp. Pharmacol.* **255**, 65–84 (2019).
8. S. G. Amara, V. Jonas, M. G. Rosenfeld, E. S. Ong, R. M. Evans, Alternative RNA processing in calcitonin gene expression generates mRNAs encoding different polypeptide products. *Nature* **298**, 240–244 (1982).
9. M. G. Rosenfeld *et al.*, Production of a novel neuropeptide encoded by the calcitonin gene via tissue-specific RNA processing. *Nature* **304**, 129–135 (1983).
10. S. D. Brain, T. J. Williams, J. R. Tippins, H. R. Morris, I. MacIntyre, Calcitonin gene-related peptide is a potent vasodilator. *Nature* **313**, 54–56 (1985).
11. F. A. Russell, R. King, S. J. Smillie, X. Kodji, S. D. Brain, Calcitonin gene-related peptide: Physiology and pathophysiology. *Physiol. Rev.* **94**, 1099–1142 (2014).
12. M. J. Gunthorpe, A. Szallasi, Peripheral TRPV1 receptors as targets for drug development: New molecules and mechanisms. *Curr. Pharm Des.* **14**, 32–41 (2008).
13. J. Sousa-Valente, S. D. Brain, A historical perspective on the role of sensory nerves in neurogenic inflammation. *Semin. Immunopathol.* **40**, 229–236 (2018).
14. R. D. Granstein, J. A. Wagner, L. L. Stohl, W. Ding, Calcitonin gene-related peptide: Key regulator of cutaneous immunity. *Acta Physiol.* **213**, 586–594 (2015).
15. P. Baral, S. Udit, I. M. Chiu, Pain and immunity: Implications for host defence. *Nat. Rev. Immunol.* **19**, 433–447 (2019).
16. F. A. Pinho-Ribeiro, W. A. Verri Jr., I. M. Chiu, Nociceptor sensory neuron-immune interactions in pain and inflammation. *Trends Immunol.* **38**, 5–19 (2017).
17. F. Hladik *et al.*, Initial events in establishing vaginal entry and infection by human immunodeficiency virus type-1. *Immunity* **26**, 257–270 (2007).
18. Y. Ganor *et al.*, Within 1 h, HIV-1 uses viral synapses to enter efficiently the inner, but not outer, foreskin mucosa and engages Langerhans-T cell conjugates. *Mucosal Immunol.* **3**, 506–522 (2010).

19. Z. Zhou *et al.*, HIV-1 efficient entry in inner foreskin is mediated by elevated CCL5/RANTES that recruits T cells and fuels conjugate formation with Langerhans cells. *PLoS Pathog.* **7**, e1002100 (2011).
20. Z. Zhou *et al.*, The HIV-1 viral synapse signals human foreskin keratinocytes to secrete thymic stromal lymphopoietin facilitating HIV-1 foreskin entry. *Mucosal Immunol.* **11**, 158–171 (2018).
21. N. Nasr *et al.*, Inhibition of two temporal phases of HIV-1 transfer from primary Langerhans cells to T cells: The role of langerin. *J. Immunol.* **193**, 2554–2564 (2014).
22. Y. Ganor *et al.*, Calcitonin gene-related peptide inhibits Langerhans cell-mediated HIV-1 transmission. *J. Exp. Med.* **210**, 2161–2170 (2013).
23. Y. Ganor, A. S. Drillet-Dangeard, M. Bomsel, Calcitonin gene-related peptide inhibits human immunodeficiency type 1 transmission by Langerhans cells via an autocrine/paracrine feedback mechanism. *Acta Physiol.* **213**, 432–441 (2015).
24. M. Bomsel, Y. Ganor, Calcitonin gene-related peptide induces HIV-1 proteasomal degradation in mucosal Langerhans cells. *J. Virol.* **91**, e01205-17 (2017).
25. J. Mariotton *et al.*, Native CGRP neuropeptide and its stable analogue SAX, but not CGRP peptide fragments, inhibit mucosal HIV-1 transmission. *Front. Immunol.* **12**, 785072 (2021).
26. E. Cohen *et al.*, CGRP inhibits human Langerhans cells infection with HSV by differentially modulating specific HSV-1 and HSV-2 entry mechanisms. *Mucosal Immunol.* **15**, 762–771 (2022).
27. V. Pena-Cruz *et al.*, HIV-1 replicates and persists in vaginal epithelial dendritic cells. *J. Clin. Invest.* **128**, 3439–3444 (2018).
28. K. M. Bertram *et al.*, Identification of HIV transmitting CD11c(+) human epidermal dendritic cells. *Nat. Commun.* **10**, 2759 (2019).
29. X. Liu *et al.*, Distinct human Langerhans cell subsets orchestrate reciprocal functions and require different developmental regulation. *Immunity* **54**, 2305–2320.e11 (2021).
30. F. Geissmann *et al.*, Transforming growth factor beta1, in the presence of granulocyte/macrophage colony-stimulating factor and interleukin 4, induces differentiation of human peripheral blood monocytes into dendritic Langerhans cells. *J. Exp. Med.* **187**, 961–966 (1998).
31. Y. Otsuka *et al.*, Differentiation of Langerhans cells from monocytes and their specific function in inducing IL-22-specific Th cells. *J. Immunol.* **201**, 3006–3016 (2018).
32. G. Picarda *et al.*, Functional langerin^{high}-expressing langerhans-like cells can arise from CD14^{high}CD16- human blood monocytes in serum-free condition. *J. Immunol.* **196**, 3716–3728 (2016).
33. D. L. Hay, M. L. Garelja, D. R. Poyner, C. S. Walker, Update on the pharmacology of calcitonin/CGRP family of peptides: IUPHAR Review 25. *Br. J. Pharmacol.* **175**, 3–17 (2018).
34. S. McGaraughty, K. L. Chu, C. R. Faltynek, M. F. Jarvis, Systemic and site-specific effects of A-425619, a selective TRPV1 receptor antagonist, on wide dynamic range neurons in CFA-treated and uninjured rats. *J. Neurophysiol.* **95**, 18–25 (2006).
35. M. Trevisani *et al.*, Ethanol elicits and potentiates nociceptor responses via the vanilloid receptor-1. *Nat. Neurosci.* **5**, 546–551 (2002).
36. H. Doods *et al.*, Pharmacological profile of BIBN4096BS, the first selective small molecule CGRP antagonist. *Br. J. Pharmacol.* **129**, 420–423 (2000).
37. M. H. Dinh *et al.*, Visualization of HIV-1 interactions with penile and foreskin epithelia: Clues for female-to-male HIV transmission. *PLoS Pathog.* **11**, e1004729 (2015).
38. E. Bodo *et al.*, Vanilloid receptor-1 (VR1) is widely expressed on various epithelial and mesenchymal cell types of human skin. *J. Invest. Dermatol.* **123**, 410–413 (2004).
39. S. Stander *et al.*, Expression of vanilloid receptor subtype 1 in cutaneous sensory nerve fibers, mast cells, and epithelial cells of appendage structures. *Exp. Dermatol.* **13**, 129–139 (2004).
40. S. Bertin *et al.*, The ion channel TRPV1 regulates the activation and proinflammatory properties of CD4(+) T cells. *Nat. Immunol.* **15**, 1055–1063 (2014).
41. S. Iyengar, M. H. Ossipov, K. W. Johnson, The role of calcitonin gene-related peptide in peripheral and central pain mechanisms including migraine. *Pain* **158**, 543–559 (2017).
42. E. S. McCoy, B. Taylor-Blake, M. J. Zylka, CGRPalpha-expressing sensory neurons respond to stimuli that evoke sensations of pain and itch. *PLoS One* **7**, e36355 (2012).
43. R. Zhang *et al.*, Sirtuin6 inhibits c-triggered inflammation through TLR4 abrogation regulated by ROS and TRPV1/CGRP. *J. Cell Biochem.* **119**, 9141–9153 (2018).
44. B. M. Assas, M. H. Wakid, H. A. Zakai, J. A. Miyan, J. L. Pennock, Transient receptor potential vanilloid 1 expression and function in splenic dendritic cells: A potential role in immune homeostasis. *Immunology* **147**, 292–304 (2016).
45. B. M. Assas, J. I. Pennock, J. A. Miyan, Calcitonin gene-related peptide is a key neurotransmitter in the neuro-immune axis. *Front. Neurosci.* **8**, 23 (2014).
46. R. K. Majhi *et al.*, Functional expression of TRPV channels in T cells and their implications in immune regulation. *FEBS J.* **282**, 2661–2681 (2015).
47. A. C. Steinberg, I. A. Oyama, A. E. Rejba, S. Kellogg-Spadt, K. E. Whitmore, Capsaicin for the treatment of vulvar vestibulitis. *Am. J. Obstet. Gynecol.* **192**, 1549–1553 (2005).
48. R. Akel, C. E. Cohen, C. Fuller, Caution with topical capsaicin. *Clin. Exp. Dermatol.* **45**, 739 (2020).
49. W. D. Rollyson *et al.*, Bioavailability of capsaicin and its implications for drug delivery. *J. Control. Release* **196**, 96–105 (2014).
50. V. Guichard *et al.*, Calcium-mediated shaping of naive CD4 T-cell phenotype and function. *Elife* **6**, e27215 (2017).

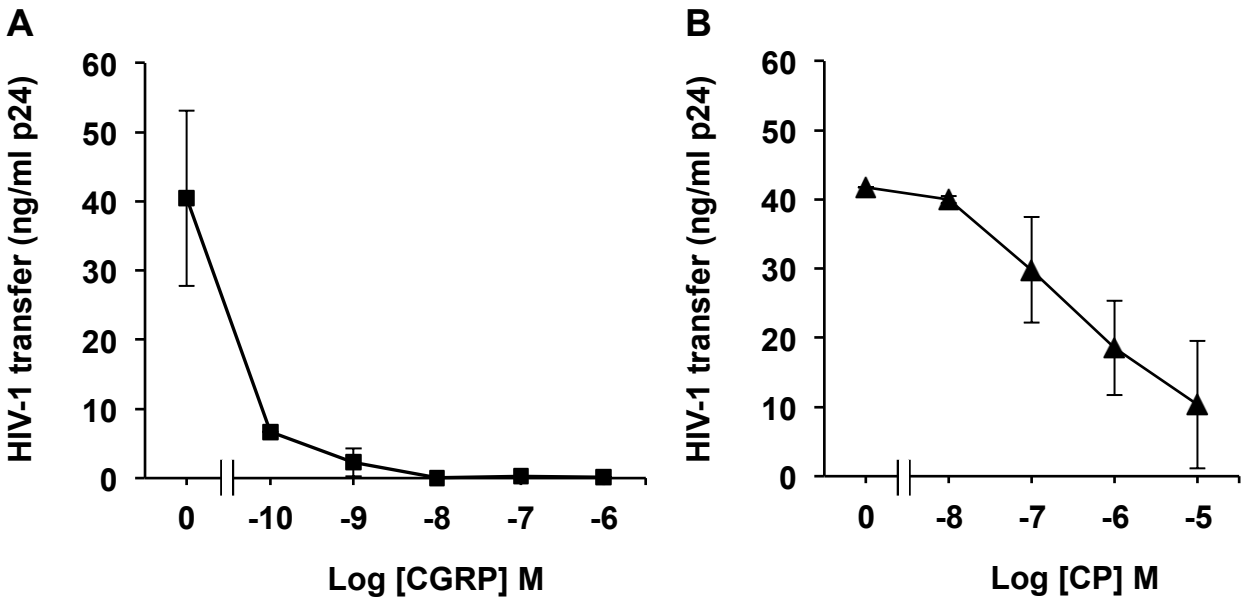

Supplementary Figure 1. CGRP and CP inhibit human MDLCs-mediated HIV-1 transfer to CD4$^+$ T-cells. MDLCs were left untreated or pre-treated for 24hr with CP **(A)** or CGRP **(B)** at the indicated molar concentrations. The cells were then washed, pulsed with HIV-1 ADA for 4h, washed again, and incubated for 7 days with autologous CD4+ T-cells. HIV-1 transfer to and resulting replication in T-cells was evaluated by p24 ELISA in the co-culture supernatants. Show are mean±SEM ng/ml levels of p24 from triplicate wells using MDLCs prepared from a healthy individual, of a representative experiment of n=3 performed.

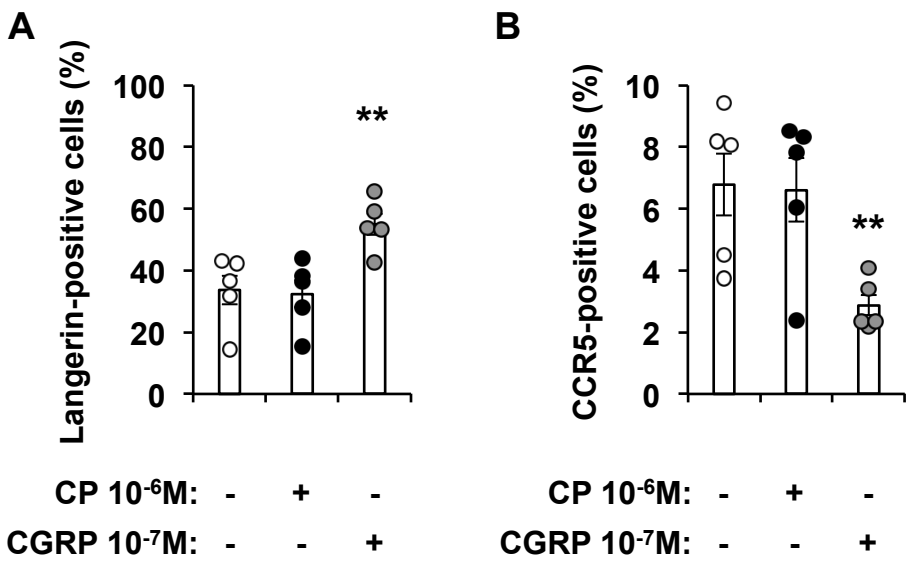

Supplementary Figure 2. CGRP, but not CP, increases langerin and decreases CCR5 surface expression in MDLCs. MDLCs were left untreated or treated for 24hr with CGRP or CP. The cells were then labeled for surface expression of langerin and CCR5, and examined by flow cytometry. Shown are mean±SEM (bars) percentages of positive cells, out of total cells **(A)**, or gated on langerin^{+} cells **(B)**. Each circle represents a distinct experiment using cells prepared from a different donor. **p=0.0062 for langerin and **p=0.0059 for CCR5, CGRP-treated vs. untreated MDLCs; Student's t-test.

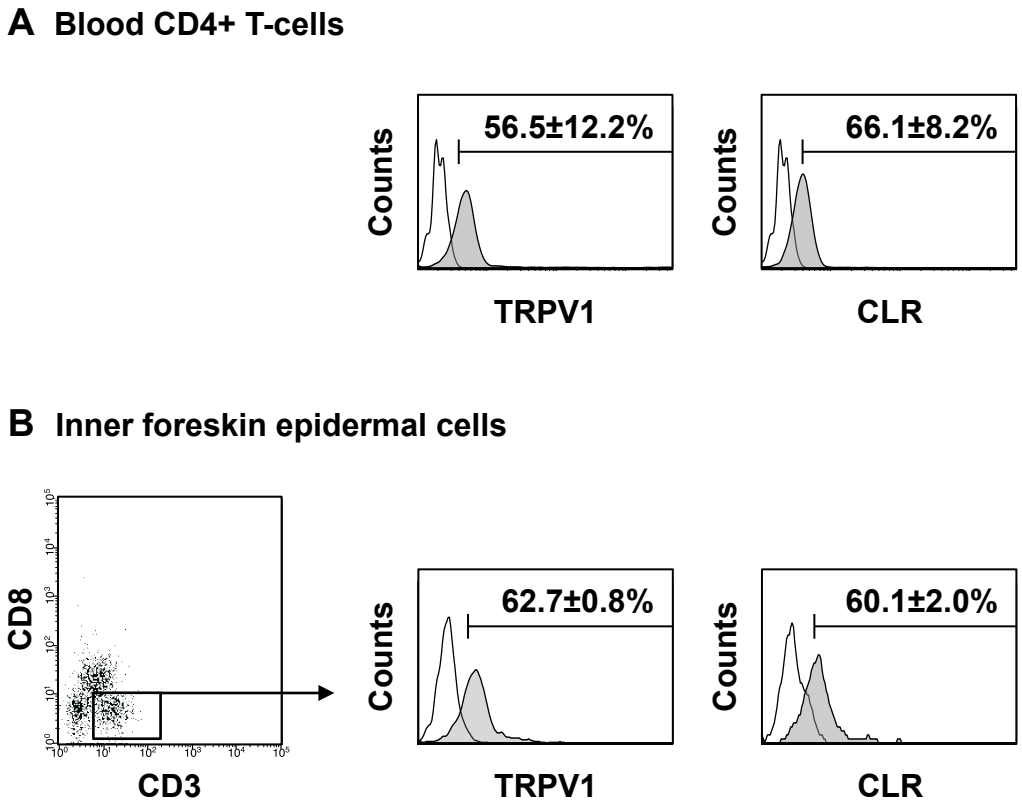

Supplementary Figure 3. Human CD4$^+$ T-cells express TRPV1 and CLR. (A) Primary human CD4$^+$ T-cells were purified from PBMCs by negative magnetic selection, labeled for surface expression of TRPV1 and CLR, and examined by flow cytometry. Representative overlays show specific staining (filled grey histograms) vs. isotype controls (broken lines); numbers represent mean±SEM (of n=3 donors tested) percentages of positive cells. **(B)** Inner foreskin epidermal cell suspensions were prepared using dispase / trypsin enzymatic digestion, labeled with Viobility Fixable Dye followed by surface expression of CD45, CD3, CD8 and TRPV1 or CLR, and examined by flow cytometry. Representative dot plot shows CD3$^+$CD8$^-$ T-cells (gated on viable CD45$^+$ cells), and overlays show specific staining (filled grey histograms) vs. isotype controls (broken lines); numbers represent mean±SEM (of n=3 tissues tested) percentages of positive cells.